Cellular/Molecular

Inositol Triphosphate-Mediated Ca^{2+} Signals Direct Purinergic P2Y Receptor Regulation of Neuronal Ion Channels

Oleg Zaika,[1] Gleb P. Tolstykh,[1] David B. Jaffe,[2] and Mark S. Shapiro[1]

[1]Department of Physiology, University of Texas Health Science Center at San Antonio, San Antonio, Texas 78229, and [2]Department of Biology, Division of Life Sciences, The University of Texas at San Antonio, San Antonio, Texas 78249

Purinergic P2Y receptors are one of four types of $G_{q/11}$-coupled receptors in rat superior cervical ganglia (SCG) sympathetic neurons. In cultured SCG neurons, purinergic and bradykinin suppression of I_M were similar in magnitude and somewhat less than that by muscarinic agonists. The effects of the P2Y receptor agonist UTP on neuronal excitability and discharge properties were studied. Under current clamp, UTP increased action potential (AP) firing in response to depolarizing current steps, depolarized the resting potential, decreased the threshold current required to fire an AP, and decreased spike-frequency adaptation. These effects were very similar to those resulting from bradykinin stimulation and not as profound as from muscarinic stimulation or full M-current blockade. We then examined the P2Y mechanism of action. Like bradykinin, but unlike muscarinic, purinergic stimulation induced rises in intracellular $[Ca^{2+}]_i$. Tests using expression of IP_3"sponge" or IP_3 phosphatase constructs implicated IP_3 accumulation as necessary for purinergic suppression of I_M. Overexpression of wild-type or dominant-negative calmodulin (CaM) implicated Ca^{2+}/CaM in the purinergic action. Both sets of results were similar to bradykinin, and opposite to muscarinic, suppression. We also examined modulation of Ca^{2+} channels. As for bradykinin, purinergic stimulation did not suppress I_{Ca}, unless neuronal calcium sensor-1 (NCS-1) activity was blocked by a dominant-negative NCS-1 construct. Our results indicate that P2Y receptors modulate M-type channels in SCG cells via IP_3-mediated $[Ca^{2+}]_i$ signals in concert with CaM and not by depletion of phosphatidylinositol-4, 5-biphosphate. We group purinergic P2Y and bradykinin B_2 receptors together as having a common mode of action.

Key words: **M current; calcium channel; purinergic receptor; PLC signaling; G-protein; patch clamp; sympathetic neuron**

Introduction

The M-type K^+ current is a prime regulator of neuronal excitability wherever its constituent Kv7 (*KCNQ*) gene products are expressed (Cooper and Jan, 2003). M-current suppression thus causes increased action potential (AP) firing and bursting, whereas its augmentation inhibits neuronal discharge (Wang et al., 1998; Peretz et al., 2005; Gamper et al., 2006; Yue and Yaari, 2006; Zaika et al., 2006). Although the critical regulatory action of transmitters on M-type channels centers on binding to membrane phosphatidylinositol 4,5-bisphosphate (PIP_2), two major modes of inhibition of M-type channels by stimulation of $G_{q/11}$-coupled receptors have emerged that use partly distinct, and partly shared, intracellular mechanisms. Both involve activation of phospholipase C (PLC) and hydrolysis of PIP_2 but differ in the use of IP_3-mediated release of Ca^{2+} from stores, subsequent $[Ca^{2+}]_i$ signals and calmodulin action (Delmas and Brown, 2005). Four $G_{q/11}$-coupled receptors have been characterized in superior cervical ganglion (SCG) sympathetic neurons: muscarinic M_1, angiotensin AT_1, bradykinin (BK) B_2, and purinergic P2Y. Muscarinic and angiotensin stimulation do not elicit $[Ca^{2+}]_i$ signals and suppress M current by PIP_2 depletion (Shapiro et al., 1994; Suh and Hille, 2002; Zhang et al., 2003; Zaika et al., 2006). Conversely, bradykinin suppression involves Ca^{2+}/CaM binding to the channels (Gamper and Shapiro, 2003), which may lower their affinity for PIP_2, but such B_2 receptor stimulation does not strongly lower global PIP_2 abundance (Gamper et al., 2004; Winks et al., 2005; Gamper and Shapiro, 2007; Hughes et al., 2007). High-threshold Ca_V2 channels are also sensitive to membrane PIP_2 abundance and are inhibited during PIP_2 depletion (Wu et al., 2002; Gamper et al., 2004). Consistent with specificity among $G_{q/11}$-coupled receptors for inducing PIP_2 depletion, stimulation of M_1 and AT_1, but not B_2, receptors suppresses endogenous I_{Ca} and heterologously expressed $K_{ir}3$ current in SCG cells (Gamper et al., 2004; Winks et al., 2005).

Purinergic receptors, classified as P2X ionotropic and P2Y metabotropic, are found throughout the nervous system (Burnstock, 2006). Although the $P2Y_1$, $P2Y_2$, and $P2Y_6$ subtypes have been described in mouse and rat sympathetic ganglia (Vartian et al., 2001; Calvert et al., 2004), $P2Y_6$ seems to be primary in rat SCG (Bofill-Cardona et al., 2000), whereas the $P2Y_1$ subtype

Received April 17, 2007; revised June 28, 2007; accepted June 30, 2007.

This work was supported by National Institutes of Health–National Institute of Neurological Disorders and Stroke Grant R01 NS43394 (M.S.S.). We thank Pamela Martin for expert technical assistance and Nikita Gamper for comments on this manuscript.

Correspondence should be addressed to Mark S. Shapiro, Department of Physiology, MS 7756, University of Texas Health Science Center at San Antonio, 7703 Floyd Curl Drive, San Antonio, TX 78229. E-mail: shapirom@uthscsa.edu.

DOI:10.1523/JNEUROSCI.1739-07.2007

 0270-6474/07/278914-13$15.00/0

dominates in mammalian CNS (Moore et al., 2001). In many neuronal types, P2Y receptor stimulation depresses M current via PLC activation, but the intracellular mechanism used from that point on appears intriguingly divergent. In the rat SCG cells also studied here, the action involves intracellular Ca^{2+} signals (Bofill-Cardona et al., 2000) but does not in frog ganglia (Stemkowski et al., 2002). Moreover, in rat hippocampus, the $P2Y_1$ receptor-mediated suppression of I_M is not associated with $[Ca^{2+}]_i$ signals and is suggested to be via PIP_2 depletion (Filippov et al., 2006). In this work, we systematically investigate the action of P2Y receptor stimulation on neuronal excitability and discharge properties of rat SCG cells and its mode of action on the endogenous I_M and I_{Ca} in those cells. The purinergic signals are compared with those from muscarinic and bradykinin stimulation and show the purinergic action to increase neuronal excitability via IP_3-mediated $[Ca^{2+}]_i$ signals.

Materials and Methods

SCG neuron culture and transduction. Sympathetic neurons were isolated from the SCG of 7- to 14-d-old male rats (Sprague Dawley) and cultured for 2–4 d. Rats were anesthetized with halothane and decapitated. Neurons were dissociated using methods of Bernheim et al. (1991), plated on 4 × 4 mm glass coverslips (coated with poly-L-lysine) and incubated at 37°C (5% CO_2). Fresh culture medium containing nerve growth factor (50 ng/ml) was added to the cells 3 h after plating. In some experiments, pertussis toxin (PTX) (100 ng/ml) was added to the culture medium. For exogenous expression of cDNA constructs in SCG neurons, we used the PDS-1000/He biolistic particle delivery system ("gene gun"; Bio-Rad, Hercules, CA), as described recently (Gamper and Shapiro, 2006). Transfection efficiency was assumed to be determined by the random distribution of fired gold particles and was up to 10% of cultured neurons.

Perforated-patch electrophysiology. Pipettes were pulled from borosilicate glass capillaries (1B150F-4; World Precision Instruments, Sarasota, FL) using a Flaming/Brown micropipette puller P-97 (Sutter Instruments, Novato, CA) and had resistances of 1–4 MΩ when filled with internal solution and measured in standard bath solution. Membrane current was measured with pipette and membrane capacitance cancellation, sampled at 5 ms or 200 μs, and filtered at 1 or 2.5 kHz (for I_M and I_{Ca}, respectively) by an EPC-9 amplifier and PULSE software (HEKA/InstruTech, Port Washington, NY). In all experiments, the perforated-patch method of recording was used with amphotericin B (600 ng/ml) in the pipette (Rae et al., 1991). Amphotericin was prepared as a stock solution as 60 mg/ml in DMSO. In these experiments, the access resistance was typically 10 MΩ 5–10 min after seal formation. Cells were placed in a 500 μl perfusion chamber through which solution flowed at 1–2 ml/min. Inflow to the chamber was by gravity from several reservoirs, selectable by activation of solenoid valves (Warner Instruments, Hamden, CT). Bath solution exchange was essentially complete by <30 s. Experiments were performed at room temperature.

M currents in SCG cells were studied by holding the membrane potential at −25 mV and applying a 500 ms hyperpolarizing pulse to −60 mV every 3 s. M-current amplitude was measured at −60 mV from the decaying time course of the deactivating current sensitive to the M-channel-specific blocker XE991 [10,10-bis(4-pyridinylmethyl)-9(10*H*)-anthracenone] (Zaczek et al., 1998). UTP, BK, oxotremorine-M (oxo-M), and XE991 were used at concentrations of 10 μM, 250 nM, 10 μM, and 50 μM, respectively. To evaluate the amplitude of I_{Ca}, cells were held at −80 mV, and 15 ms depolarizing steps to 5 mV were applied every 5 s. The amplitude of I_{Ca} was usually defined as the inward current sensitive to Cd^{2+} (100 μM). The external solution used to record M currents contained the following: 150 mM NaCl, 5 mM KCl, 2 mM $CaCl_2$, 1 mM $MgCl_2$, 10 mM glucose, 10 mM HEPES, and 500 nM tetrodotoxin, pH 7.4 with NaOH. For I_{Ca} recordings, KCl was reduced to 2.5 mM, and $CaCl_2$ was increased to 5 mM. The pipette solution for voltage-clamp experiments contained the following (in mM): 150 KCl/CsCl, 5 $MgCl_2$, and 10 HEPES to record I_M/I_{Ca}. For current-clamp experiments, the pipette solution contained the following (in mM): 20 KCl, 100 K-acetate, 5 $MgCl_2$, and 40 HEPES. Data are presented as mean ± SEM. Statistical tests were performed using paired *t* test or unpaired *t* test when appropriate.

Imaging. Fluorescent microscopy was performed with an inverted Nikon (Tokyo, Japan) Eclipse TE300 microscope with an oil-immersion 40×/1.30 numerical aperture objective. A Polychrome IV monochromator (T.I.L.L. Photonics, Martinsreid, Germany) was used as the excitation light source, and a FURA2 71000 filter cube (Chroma Technology, Brattleboro, VT) was used for fura-2 imaging. SCG neurons were bath loaded with fura-2 AM (2 μM) for 30 min at 37°C in the presence of pluronic acid (0.01%). Cells were excited alternatively at 340 and 380 nm (50–200 ms every 2 s), the fluorescence emission was collected by an IMAGO 12-bit cooled CCD camera, and images were stored/analyzed with TILLvisION 4.0 software. These fura-2 signals were not calibrated because of inherent difficulties in calibrating esterified indicator dyes (Zhou and Neher, 1993).

Computer modeling. Simulations were performed using NEURON version 5.9 (Hines and Carnevale, 2001) on a Macintosh G4 computer (Apple Computers, San Jose, CA). The passive properties of a single compartment model (50 μm diameter) were chosen to reflect the input resistance and charging time constant of SCG neurons to hyperpolarizing current steps (specific membrane resistivity, 50,000 Ωcm^2; specific capacitance, 1 μF/cm^2). Four voltage-gated and two Ca^{2+}-dependent conductances (available for download through ModelDB at http://senselab.med.yale.edu) were inserted into the model. A fast voltage-gated Na^+ conductance (nahh.mod) (Traub et al., 1991) was inserted with a density of 5 mS/cm^2. Threshold was adjusted by shifting the voltage dependence of the forward and backward activation rate constants by +20 and +10 mV, respectively. Spike repolarization was achieved with a delayed rectifier K^+ conductance (kdr.mod) (Migliore et al., 1995) at a density of 0.3 mS/cm^2 (E_K of −80 mV). A high-threshold, non-inactivating voltage-gated Ca^{2+} conductance (cal.mod) (Migliore et al., 1995) at a density of 2 mS/cm^2 was inserted with E_{Ca} determined by the Goldman–Hodgkin–Katz equation. Intracellular calcium dynamics were modeled including both rapid buffering and Ca^{2+} pumps (cadifus-.mod). Two Ca^{2+}-dependent K^+ conductances were included in the model. A BK-type Ca^{2+}-dependent conductance (cagk.mod) at a density of 0.1 mS/cm^2 contributed mostly to spike repolarization, whereas an SK-type Ca^{2+}-dependent conductance (g_{SK} of 3.9 · $[Ca^{2+}]$ mS/cm^2) contributed mostly to spike-frequency adaptation (SFA). Finally, the M-channel conductance (g_M) (im.mod) (Migliore et al., 1995) was added with a density of 0.0175 mS/cm^2. It was assumed that the M current was active at rest and therefore contributed to the resting potential of the cell. Therefore, the equilibrium potential of the leak conductance was determined with no M current resulting for an initial resting potential (V_{rest}) of −50 mV. When g_M was active, V_{rest} in the model became −55 mV.

DNA constructs. Plasmids containing wild-type (wt) or dominant-negative (DN) vertebrate CaM were given to us by Trisha Davis (University of Washington, Seattle, WA). DN CaM has an alanine substitution in each of the four Ca^{2+}-binding EF hands (D20A, D56A, D93A, and D129A). DN neuronal calcium sensor-1 was given to us by Andreas Jeromin (Mt. Sinai Hospital, Toronto, Ontario, Canada). The IP_3 sponges consist of residues 224–604 of the rat type 1 IP_3 receptor containing either the R441Q ("high-affinity sponge") or K508A ("low-affinity sponge") mutations, made by PCR amplification and given to us by Llewelyn Roderick (Babraham Institute, Cambridge, UK).

Reagents. The following reagents were used: UTP, TTX, NGF, bradykinin, oxo-M, and collagenase type I (Sigma, St. Louis, MO); fura-2 AM (Invitrogen, Carlsbad, CA); DMEM, fetal bovine serum, and penicillin/streptomycin (Invitrogen); amphotericin B and PTX (Calbiochem, La Jolla, CA); and XE991 (Tocris Bioscience, Ellisville, MO).

Results

We first evaluated the effect of purinergic stimulation on the M current in cultured SCG neurons and compared it with that of muscarinic and BK stimulation. Such a comparison between the effects of stimulating these receptor types was made throughout

this study, because the muscarinic and bradykinin actions are the prototypes for the two described mechanisms of $G_{q/11}$-mediated suppression of I_M, the first being via PIP_2 depletion and second via IP_3, $[Ca^{2+}]_i$ signals, and CaM (Delmas and Brown, 2005). Cells were studied under perforated-patch voltage clamp, and agonists were applied by bath perfusion. Guided by previous work on P2Y receptor-mediated modulation of M current (I_M) in these cells (Boehm, 1998; Bofill-Cardona et al., 2000), we chose to use UTP as the purinergic agonist in this study. UTP is not an agonist of the ionotropic P2X receptors in the SCG (Calvert and Evans, 2004). Application of UTP caused a significant suppression of I_M in approximately one-half and BK in approximately three-fourths of the neurons examined, which we assume to reflect that proportion of neurons that express UTP-sensitive P2Y or BK receptors, respectively. There were no morphological differences between cells that did or did not respond to UTP. For those neurons that responded to UTP with a suppression of I_M >5%, we compared the response with those from bradykinin and the muscarinic agonist oxo-M. Application of UTP, BK, or oxo-M suppressed I_M by 54 ± 5% ($n = 6$), 62 ± 6% ($n = 6$), and 81 ± 6% ($n = 6$), respectively (Fig. 1). These values are consistent with those reported previously, although the extent of the purinergic suppression is slightly greater than that seen previously (Bofill-Cardona et al., 2000).

Purinergic and bradykinin stimulation increases neuronal excitability and decreases spike-frequency adaptation

Given the widely demonstrated control of neuronal excitability by M-current activity (Jones et al., 1995; Gu et al., 2005; Peretz et al., 2005; Peters et al., 2005; Shen et al., 2005; Gamper et al., 2006; Vervaeke et al., 2006; Yue and Yaari, 2006; Zaika et al., 2006), we next assessed the effects of purinergic stimulation on AP firing in our preparation of cultured SCG cells. We also systematically evaluated the effects of BK stimulation, whose actions on neuronal discharge have only been briefly described (Jones et al., 1995). Using perforated-patch current-clamp recording, we evaluated both the active and passive properties of the neurons in response to current steps in the presence or absence of UTP and BK. We compared the effects of UTP and BK with the well described M-current-mediated effects of muscarinic agonists or M-channel blockade. PTX was not used, meaning that $G_{q/11}$-mediated actions are not isolated in these experiments. Because our initial voltage-clamp experiments suggested that only approximately half of the neurons express the P2Y receptor, we triaged the cells studied under current clamp so as to characterize only P2Y receptor-expressing neurons. For each neuron studied, the resting potential (V_{rest}) was monitored for 10 min before application of any agonist. During application of UTP, if V_{rest} changed outside of the range seen during that 10 min control period, we assumed that neuron to express P2Y receptors, and the cell was studied further. As for the voltage-clamp experiments, approximately half of the neurons satisfied that criterion.

Shown in Figure 2 are representative voltage recordings in response to positive or negative current steps. In control, a 100 pA current injection elicited a short train of APs that terminated well before the end of the current step (Fig. 2*A*). Application of UTP caused a reversible increase in the number of APs elicited by the 100 pA current step, consistent with suppression of M current (Fig. 2*B*,*C*). Subsequent application of BK also caused a reversible increase in AP firing that was slightly greater than that caused by UTP (Fig. 2*D*,*E*). Finally, the response to muscarinic stimulation was a spike train that was nearly as intense as that caused by total blockade of M channels by the selective blocker XE991 (Fig. 2*F*,*G*). In control, the number of APs elicited by the 2 s, 100 pA depolarizing current was 4.1 ± 1.2 ($n = 14$). Application of UTP, BK, oxo-M, or XE991 increased the number of such APs to 7.8 ± 0.9 ($p < 0.01$; $n = 9$), 8.7 ± 0.8 ($p < 0.01$; $n = 11$), 20.2 ± 0.8 ($p < 0.001$; $n = 12$), or 22.0 ± 1.8 ($p < 0.001$; $n = 12$), respec-

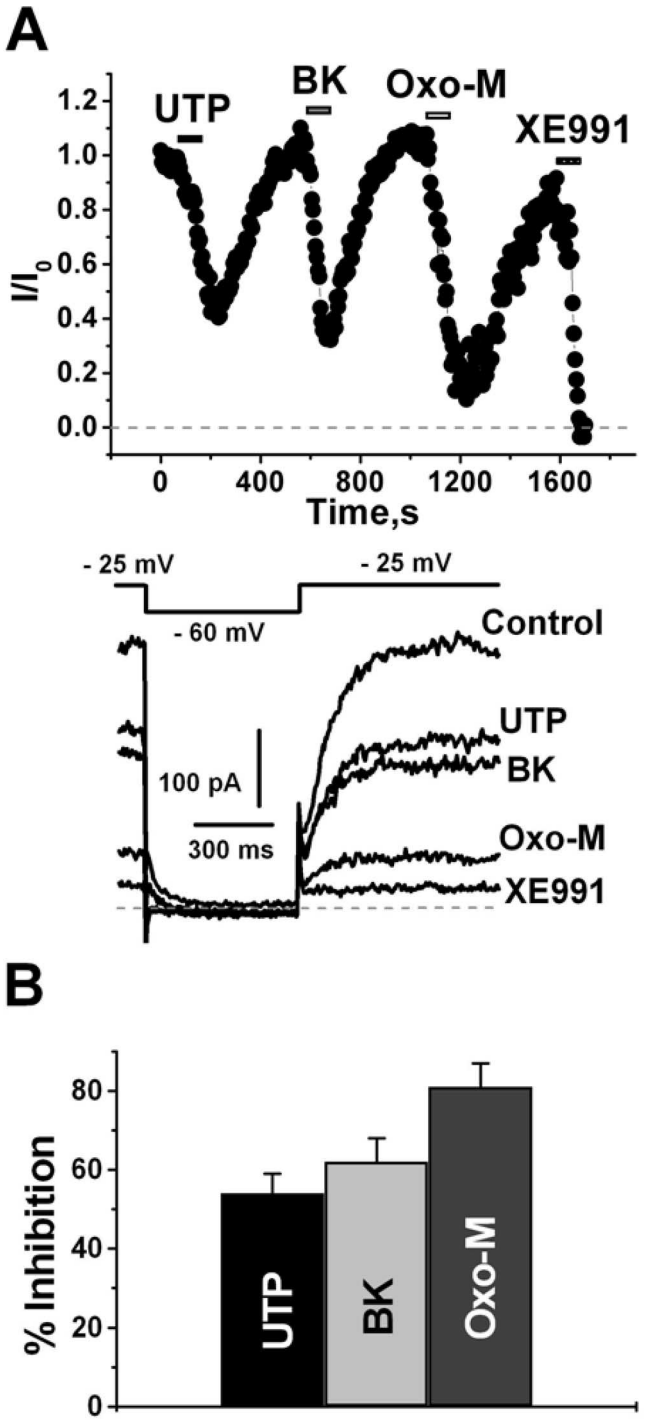

Figure 1. Purinergic stimulation suppresses M current in SCG neurons. Purinergic inhibition of M current recorded from cultured SCG neurons using the pulse protocol depicted in the inset. ***A***, Plotted are normalized M-current amplitudes, quantified as the deactivating time-dependent relaxations at −60 mV from pulses given every 3 s. UTP (10 μM), BK (250 nM), oxo-M (10 μM), or XE991 (50 μM) were bath applied during the periods shown by the bars and representative current traces shown below. ***B***, Bars show mean inhibitions of I_M by UTP, BK, or oxo-M.

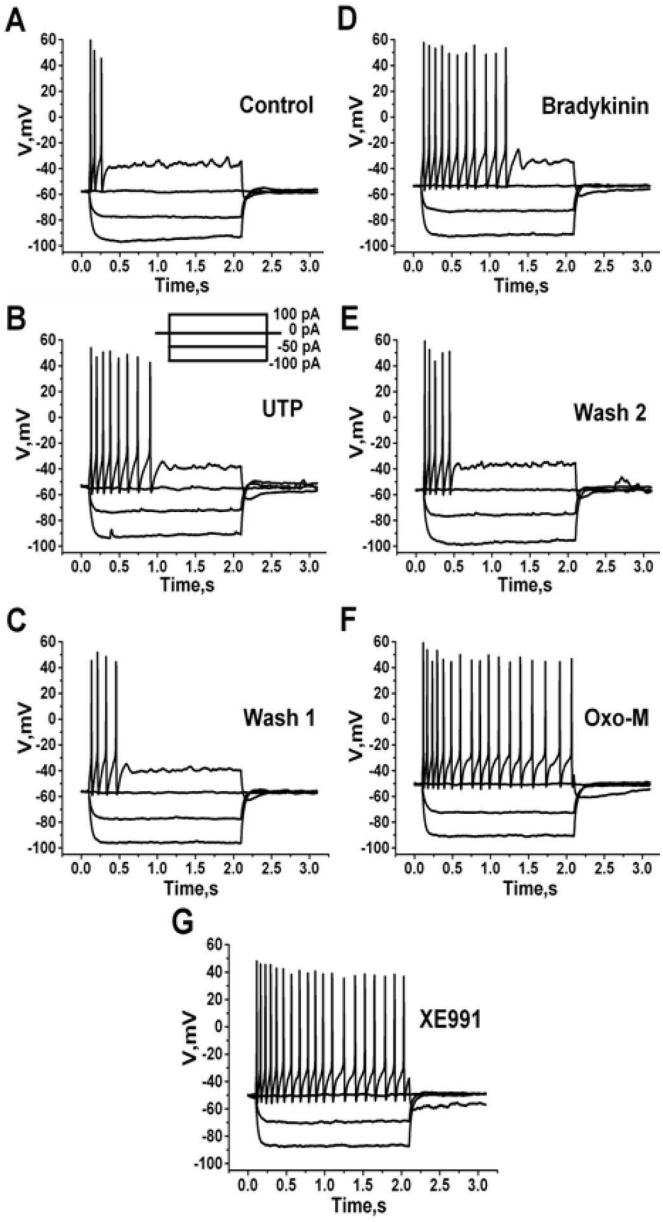

Figure 2. Purinergic stimulation increases action potential firing in SCG neurons. Cultured SCG neurons were studied under perforated-patch current clamp, and voltages were recorded from a family of current pulses (inset). Voltage sweeps are shown in control (***A***), after UTP (10 μM) (***B***), first wash (***C***), after BK (250 nM) (***D***), second wash (***E***), after oxo-M (10 μM) (***F***), or after XE991 (50 μM) (***G***).

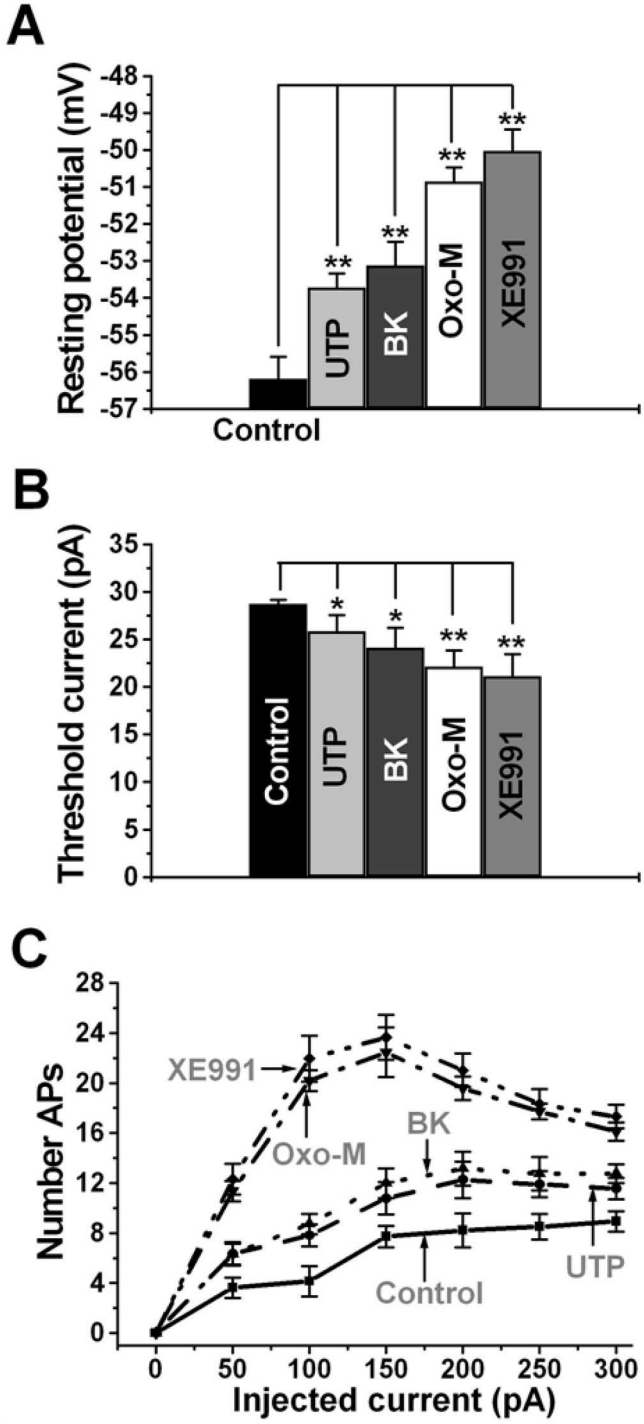

Figure 3. Control of somatic excitability by regulation of M current. Bars show summarized data of the resting potential (***A***) and the threshold current required for firing of action potentials (***B***) for SCG neurons in control, after UTP (10 μM), BK (250 nM), oxo-M (10 μM), or XE991 (50 μM). ***C***, Plotted are the number of APs elicited during a 2 s depolarizing current injection over a range of current amplitudes, during the indicated conditions. $^*p < 0.05$; $^{**}p < 0.01$.

tively. There was not a significant change in the responses to hyperpolarizing current steps, ruling out an effect of the agonists on inward conductances such as I_h.

The effect of receptor stimulation on V_{rest} was quantified as an initial indictor of control over excitability (Fig. 3*A*). In control, V_{rest} was -56.2 ± 0.6 mV ($n = 14$). Application of UTP or BK modestly depolarized V_{rest} to -53.7 ± 0.4 mV ($p < 0.01$; $n = 9$) and -53.1 ± 0.6 mV ($p < 0.01$; $n = 11$), respectively. In some experiments, we tested the effect of BK applied first to rule out any residual effect of previous UTP application, and, in those cells, the initial V_{rest} was -55.7 ± 0.3 mV, which was depolarized by BK to -53.4 ± 0.1 mV ($p < 0.01$; $n = 12$), similar to the effect of BK in cells in which UTP was applied first. Application of oxo-M induced a stronger depolarization of V_{rest}, to -50.9 ± 0.4 mV ($p < 0.01$; $n = 12$), nearly as much as that induced by XE991 (-50.0 ± 0.6 mV; $p < 0.01$; $n = 12$). We further quantified the effects of stimulation of $G_{q/11}$-coupled receptors on excitability by examining the relationship between injected current and AP firing (Fig. 3*B*,*C*). In control, the amplitude of the current re-

quired to reach threshold for AP generation (AP_{thresh}) was 28.8 ± 0.4 pA ($n = 20$). Application of UTP or BK modestly decreased AP_{thresh} to 25.9 ± 1.7 pA ($p < 0.05$; $n = 9$) and 24.1 ± 2.1 pA ($p < 0.05$; $n = 11$), respectively. Application of oxo-M reduced AP_{thresh} more strongly, to 22.1 ± 1.7 pA ($p < 0.01$; $n = 12$), nearly as much as from full M-channel blockade by XE991 (21.1 ± 2.3 pA; $p < 0.01$; $n = 12$). Evaluated over a range of current amplitudes, UTP and BK modestly, but significantly, increased the number of elicited APs at all amplitudes of injected current (Fig. 3*C*). The effect of muscarinic stimulation was stronger and was nearly as great as that produced by XE991. In summary, purinergic and BK stimulation both suppressed I_M by 50–60%, and both modestly, but significantly, increased somatic excitability to a similar degree.

Many neurons, including ganglia cells, exhibit SFA, characterized by the slowing or cessation of AP firing during a maintained stimulatory input. M current has been shown to be a prime contributor to SFA because of its accumulating conductance as the slowly activating M channels turn on during a spike train (Lawrence et al., 2006; Vervaeke et al., 2006; Zaika et al., 2006). We evaluated the effect of P2Y or BK receptor stimulation on SFA during a train of spikes using two related measures: (1) the relationship between interspike interval and spike number, and (2) spike-train duration (Fig. 4*A*). Spike trains elicited by 100 pA stimulatory currents were analyzed from SCG neurons studied under perforated-patch current clamp. In control, the instantaneous interspike interval rapidly lengthened during the short spike train, which terminated after 0.4 ± 0.1 s ($n = 14$). In the presence of UTP or BK, the slope of the interspike interval versus spike number relationship was significantly more shallow, and the spike-train duration was lengthened to 1.2 ± 0.1 s ($p < 0.01$; $n = 9$) and 1.3 ± 0.1 s ($p < 0.01$; $n = 11$), respectively. In accord with its greater effect on I_M and on AP firing, muscarinic stimulation more greatly dampened SFA, resulting in a very shallow relationship between interspike interval and spike number, and a spike-train duration that was lengthened to 1.8 ± 0.1 s ($p < 0.001$; $n = 12$). Complete blockade of M channels by application of XE991 made that relationship only slightly shallower and resulted in a spike train that lasted throughout the length of the 2 s stimulatory pulse.

In a recent paper, we used a multi-conductance neuronal model to successfully predict the effects on AP firing and SFA of suppression of M-channel conductance by angiotensin II (Zaika et al., 2006). The model program, NEURON version 5.7 (Hines and Carnevale, 2001), contains four voltage-gated and two Ca^{2+}-dependent conductances, including g_M (Borg-Graham, 1991; Migliore et al., 1995). In the study by Zaika et al. (2006), we included only a BK conductance as a K_{Ca} type, but here we also include an SK conductance in the simulation. The values of the six conductances were adjusted to best correlate with the observed behavior of the neurons (for details, see Materials and Methods). In the model, full activity of both SK- and M-type conductances resulted in a response to a depolarizing current of only several APs, but turning off of M current (at first leaving the SK current intact) changed the response to an uninterrupted spike train exhibiting only minimal SFA (data not shown), similar to what we observed (Fig. 2*A*,*G*). In Figure 4*B* are shown the predictions of the model for the interspike interval versus spike number relationship and spike-train duration over a range of fractional g_M activation. We examined these model data to see whether the effects on SFA correlate with the degree of suppression of I_M for the agonists used in this study. In comparing Figure 4, A_1 and B_1, one can see that the predicted interspike interval

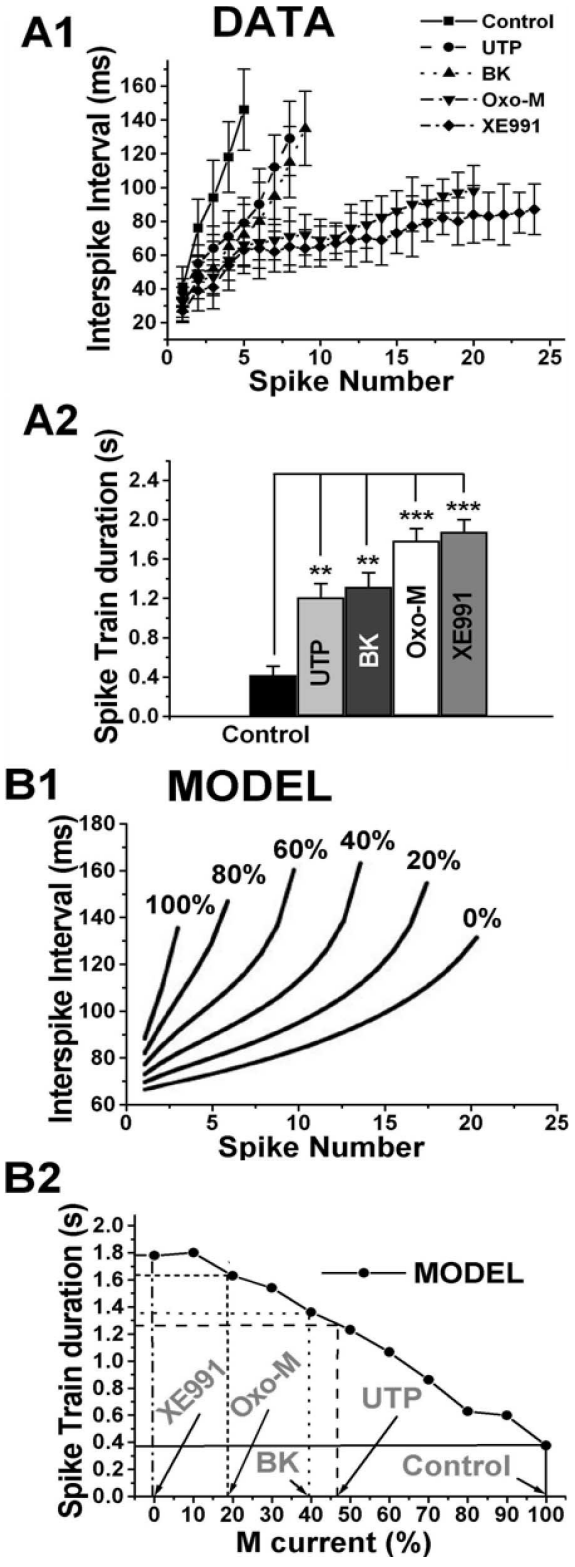

Figure 4. Effects on spike-frequency adaptation and comparison with a computer model of neuronal discharge. Plotted are the instantaneous interspike interval as a function of spike number (***A1***) and spike-train duration (***A2***) from spike trains elicited by a 100 pA stimulus applied to SCG neurons under current clamp, in control, after UTP (10 μM), BK (250 nM), oxo-M (10 μM), and XE991 (50 μM). In ***B1*** are shown the simulated curves of interspike interval versus spike number predicted by a neuronal discharge model over the indicated range of fractional M-current activity. In ***B2*** are plotted the simulated dependence of spike-train duration on fractional M-current activity. The observed suppressions of M current by the compounds used in this paper are marked on the abscissa and the predicted spike-train durations on the ordinate for comparison with the data in ***A2***. $^{**}p < 0.01$, $^{***}p < 0.001$.

versus spike number relationships at 100, 60, 20, and 0% g_M qualitatively match the experimentally observed relationships for control, UTP ≈ BK, oxo-M, and XE991, under which conditions the fractional I_M is 100, 38–46, 18, and 0%, respectively. Indicated on the model predictions of spike-train durations are the measured suppressions of I_M and the predicted spike-train durations as a result (Fig. 4B_2). For control, UTP, BK, oxo-M, and XE991, the predicted spike-train durations are ~0.4, 1.25, 1.35, 1.65, and 1.8 s, which qualitatively agree with the experimentally observed values (Fig. 4A_2).

With the SK conductance included, the model prediction of spike-train duration versus g_M includes an inflection in the curve at ~10% g_M, which the model ascribes to an oscillation in the membrane potential from sequential SK-induced hyperpolarization, turning off of M current, depolarization that produces rises in $[Ca^{2+}]_i$ via influx through Ca^{2+} channels, and cycling back to the turning on of SK channels. We observed such membrane oscillations of 2–3 mV in many of our current-clamp recordings, although this phenomenon was not studied further. The reduction of SFA produced by muscarinic stimulation, as measured by the interspike interval versus spike number relationship, was somewhat greater than that predicted by M-current suppression alone, especially at spike numbers >15, in which the model predicts an upward inflection as opposed to the flat relationship actually observed. This is likely attributable to concurrent suppression of I_{Ca} by M_1 and M_4 receptor stimulation and consequential reduction in K_{Ca} conductances. Indeed, systematic reduction of I_{SK} in the model reduced SFA for later spikes of a given train. As a result, when g_M was 20% of control, reducing I_{SK} or I_{Ca} resulted in SFA that approached that of 0% g_M, as observed experimentally.

P2Y receptor stimulation induces intracellular Ca^{2+} signals and requires IP_3 for suppression of I_M

In SCG neurons, stimulation of bradykinin B_2, but not muscarinic M_1 nor angiotensin AT_1, receptors induce $[Ca^{2+}]_i$ signals from IP_3-gated stores (Delmas et al., 2005). Although all three receptor types couple to $G_{q/11}$ and activate phospholipase C, it is hypothesized that colocalization of B_2, but not M_1 or AT_1, receptors with IP_3 receptors in "microdomains" accounts for this selectivity for eliciting $[Ca^{2+}]_i$ signals (Delmas and Brown, 2002; Delmas et al., 2002). Previous work has demonstrated P2Y receptor-mediated suppression of I_M to be via $G_{q/11}$ and to require PLC activity (Bofill-Cardona et al., 2000; Stemkowski et al., 2002). We thus began our investigation of the intracellular mechanism linking P2Y receptor stimulation with suppression of I_M by asking whether UTP elicits $[Ca^{2+}]_i$ signals in SCG neurons. $[Ca^{2+}]_i$ changes were observed using fura-2 loaded into the cells via the bath solution as the AM ester. We tested the ability of UTP, as well as BK and oxo-M, to provoke Ca^{2+} signals. Only cells in which the resting 340/380 nm ratio was <0.3 were used in these measurements. Although the cells were not voltage clamped, the bath contained TTX to eliminate the possibility of $[Ca^{2+}]_i$ rises caused by AP spiking and Ca^{2+} influx through Ca_V channels attributable to agonist-induced depolarization of V_{rest}. Shown in Figure 5*A* is a representative experiment from two adjoining SCG neurons. The 340/380 nm ratio is shown pseudocolored using the indicated scale. Muscarinic stimulation with oxo-M did not result in a measurable $[Ca^{2+}]_i$ signal, but subsequent application of UTP caused an obvious and reversible rise in $[Ca^{2+}]_i$ that was not as large as that induced by BK. In such experiments, the resting 340/380 nm ratio was 0.21 ± 0.01 (n = 20), and the rises in the 340/380 nm ratio evoked by application of oxo-M, UTP, and BK were 0.016 ± 0.002 (n = 6), 0.10 ± 0.02 (n = 7), and 0.31 ± 0.03 (n = 15), respectively (Fig. 5*B*). Our data indicate that, like bradykinin but unlike muscarinic agonists (Cruzblanca et al., 1998), purinergic P2Y receptor agonists induce rises in intracellular Ca^{2+} in sympathetic ganglia cells.

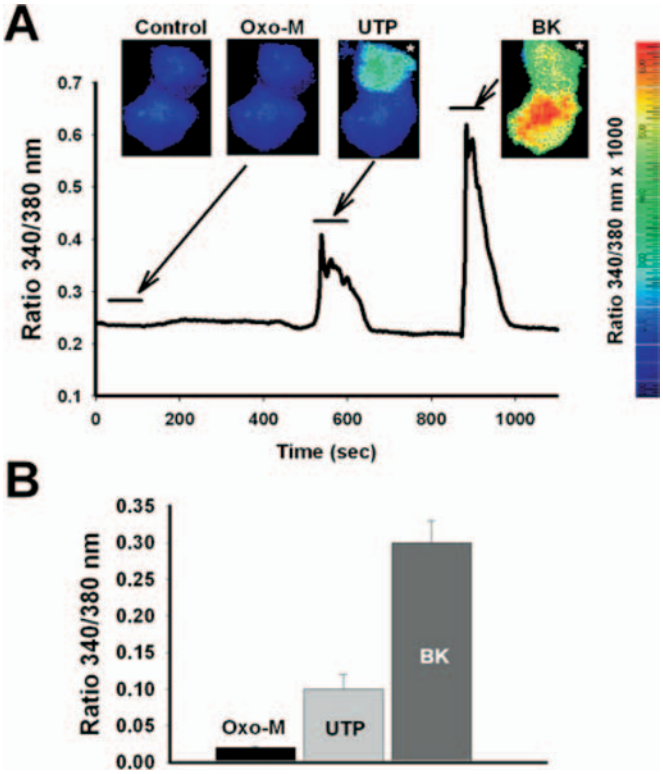

Figure 5. Purinergic stimulation induces intracellular Ca^{2+} signals. Shown in ***A*** is a representative experiment from two SCG neurons loaded with fura-2 dye from the bath as the AM ester. Shown are pseudocolor 340/380 nm ratio images of fura-2 fluorescence from two adjoining neurons in control and during 2 min applications of oxo-M (10 μM), UTP (10 μM), and BK (250 nM). The pseudocolor scale runs from blue (low $[Ca^{2+}]$) to red (high $[Ca^{2+}]$). Plotted is the 340/380 nm ratio during the experiment for the topmost neuron (white asterisk). The agonists were applied during the indicated times. Bars in ***B*** are the summarized results of these experiments.

P2Y receptor stimulation requires IP_3 and functional CaM for suppression of I_M

We then probed for the involvement of IP_3 in UTP-induced suppression of I_M. Our first test used a construct containing a fusion protein of enhanced green fluorescent protein (EGFP) and point mutants of the IP_3-binding domain in the N-terminal of the rat type 1 IP_3 receptor. A protein consisting only of residues 224–604 has an affinity for IP_3 in the range of 92 pM and the R441Q mutant 45 pM, some 1000-fold higher than the native IP_3 receptor, whereas the K508A mutant reduces the affinity to only 340 nM. The R441Q, but not the K508A, mutant has been shown to be an effective sponge of IP_3 when overexpressed in cells, preventing accumulation of IP_3 in the cytoplasm during PLC activation and any downstream $[Ca^{2+}]_i$ signal (Uchiyama et al., 2002). Transfection of SCG neurons was performed using a biolistic particle delivery device (gene gun), using recently described procedures (Gamper and Shapiro, 2006), and the neurons were studied the following day under perforated-patch voltage clamp. Figure 6, *A* and *B*, shows experiments on neurons transfected with either the K508A low-affinity sponge or the R441Q high-affinity sponge.

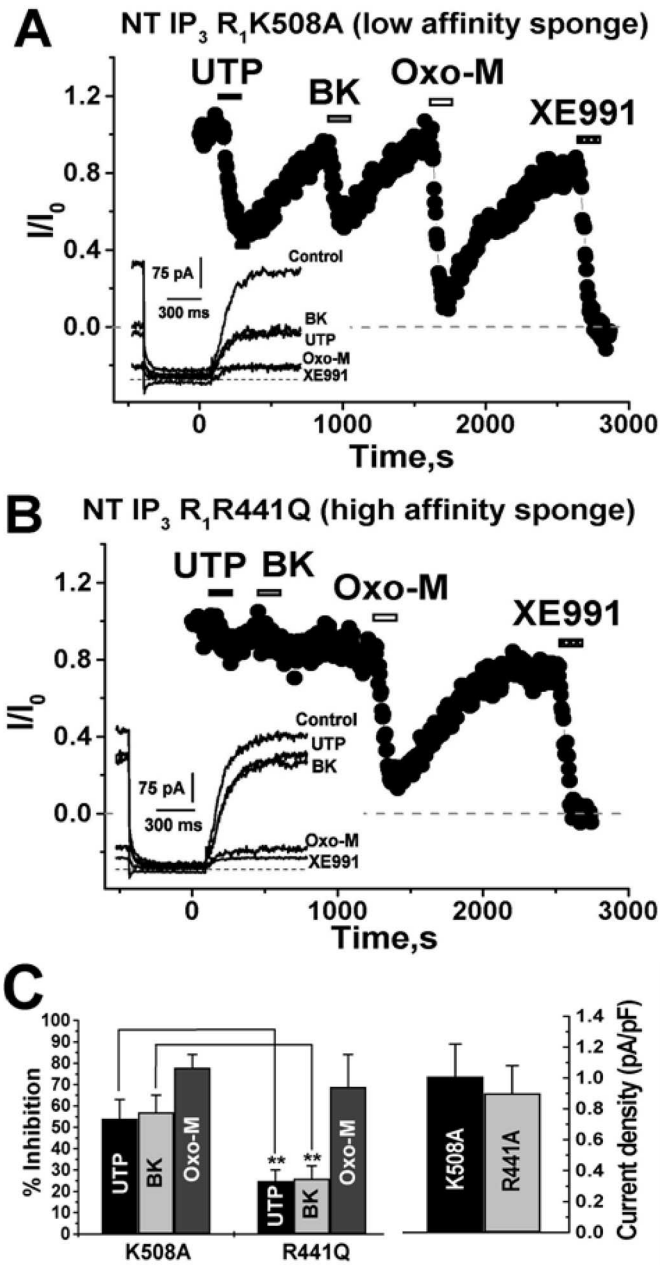

Figure 6. A high-affinity IP_3 sponge blocks purinergic inhibition of M current. Plotted are normalized M-current amplitudes, quantified as before, from neurons transfected with the N-terminal IP_3 type 1 receptor (NT IP_3R_1) K508A low-affinity sponge (***A***) or the N-terminal IP_3R_1 R441Q high-affinity sponge (***B***) using the gene gun and studied using perforated-patch recording. UTP (10 μM), BK (250 nM), oxo-M (10 μM), or XE991 (50 μM) were bath applied during the periods shown by the bars. Representative current traces during the experiments are shown in the insets. ***C***, Bars show summarized inhibitions by UTP, BK, or oxo-M (left) or tonic I_M densities (right) for cells transfected with the low-affinity (K508A) or the high-affinity (R441Q) sponges. $^{**}p < 0.01$.

Whereas the cell overexpressing the low-affinity sponge displayed robust and reversible suppressions of I_M by UTP, BK, and oxo-M, the cell overexpressing the high-affinity sponge responded to both UTP and BK with very little suppressions of I_M, but the response to oxo-M was unaltered. These data are summarized in Figure 6*C* (left). In neurons transfected with the low-affinity sponge, the suppressions of I_M by UTP, BK, and oxo-M were 54 ± 9% ($n = 5$), 57 ± 8% ($n = 6$), and 78 ± 6% ($n = 6$), respectively. In neurons transfected with the high-affinity sponge, the suppressions of I_M by UTP, BK, and oxo-M were 25 ± 5% ($p < 0.01$; $n = 5$), 26 ± 6% ($p < 0.01$; $n = 8$), and 69 ± 15% ($n = 8$). There was no effect on tonic I_M densities of sponge expression (Fig. 6*C*, right). In neurons transfected with the K508A sponge or the R441Q sponge, tonic I_M densities were 1.0 ± 0.2 and 0.9 ± 0.2 pA/pF ($n = 6$ and 8), respectively. As another test to determine which receptor types require IP_3 accumulation for suppression of I_M, we assayed the effects of overexpression of a type 1 IP_3-5′phosphatase (IP_3-P), whose activity is the first step in IP_3 degradation. Overexpression of IP_3-P results in rapid dephosphorylation of IP_3 molecules as soon as they are made, preventing its accumulation in the cytoplasm (Hirose et al., 1999). As for the IP_3 sponge experiments, the constructs were transfected into SCG neurons using the gene gun and studied under perforated-patch voltage clamp. Figure 7, *A* and *B*, shows experiments on a control neuron transfected only with EGFP or a neuron cotransfected with EGFP-tagged IP_3-P. Whereas the control neuron displayed robust and reversible suppressions of I_M by UTP, BK, and oxo-M, the neuron overexpressing IP_3-P responded to both UTP and BK with suppressions of I_M that were very weak, but the response to oxo-M was still large.

Along with the involvement of IP_3-mediated $[Ca^{2+}]_i$ signals in suppression of I_M by bradykinin is the use of CaM as the Ca^{2+} sensor of M channels. Much like the role of CaM in Ca^{2+}-dependent inactivation of Ca_V channels (Halling et al., 2006) and activation of SK-type K^+ channels (Maylie et al., 2004), CaM binds to M-type channels and inhibits them on $[Ca^{2+}]_i$ signals, perhaps by reducing the affinity of PIP_2 for the channels (Brown et al., 2007). Given the role of IP_3 in the purinergic action shown here, we therefore tested for the involvement of CaM in UTP-mediated suppression of I_M. SCG neurons were transfected with either wt CaM or a DN CaM that has an Asp-to-Ala mutation in all four Ca^{2+}-binding sites, rendering it unable to bind Ca^{2+} (Geiser et al., 1991). If $[Ca^{2+}]_i$ signal sensing by CaM mediates purinergic inhibition of M channels, then we predict overexpression of DN CaM to block the suppression because channels will be bound by CaM molecules that cannot sense $[Ca^{2+}]_i$, and we would predict overexpression of wt CaM to amplify tonic Ca^{2+}/CaM modulation because many channels would be bound by Ca^{2+}/CaM at resting $[Ca^{2+}]_i$ (Gamper and Shapiro, 2003). Figure 7*C* shows an experiment on a neuron overexpressing DN CaM. In this cell, the suppression of I_M in response to application of UTP or BK was negligible but that from oxo-M application was robust. In Figure 7*D*, an experiment on a neuron overexpressing wt CaM is shown, in which the responses to UTP and BK were very small and that from oxo-M application was somewhat attenuated.

The suppressions of I_M in these four groups of cells are summarized in Figure 7*E* (left). In neurons transfected only with EGFP, the suppressions of I_M by UTP, BK, and oxo-M were 58 ± 8% ($n = 7$), 61 ± 6% ($n = 9$), and 80 ± 5% ($n = 9$), indistinguishable from nontransfected cells. However, in cells transfected with IP_3-P, the suppressions of I_M by UTP and BK, but not oxo-M, were severely blunted, with responses to UTP, BK, and oxo-M of 22 ± 8% ($p < 0.01$; $n = 5$), 23 ± 7% ($p < 0.01$; $n = 6$), and 71 ± 9% ($n = 6$), respectively. Likewise, in cells transfected with DN CaM, only the suppression of I_M by oxo-M remained intact. Thus, the responses to UTP, BK, and oxo-M were 18 ± 5% ($p < 0.01$; $n = 5$), 20 ± 4% ($p < 0.01$; $n = 5$), and 82 ± 7% ($n = 5$), respectively. The fractional suppressions of I_M by UTP and BK were also sharply reduced and that by oxo-M somewhat attenuated in cells overexpressing wt CaM. In those cells, the responses to UTP, BK, and oxo-M were 21 ± 5% ($p < 0.01$; $n = 4$), 23 ±

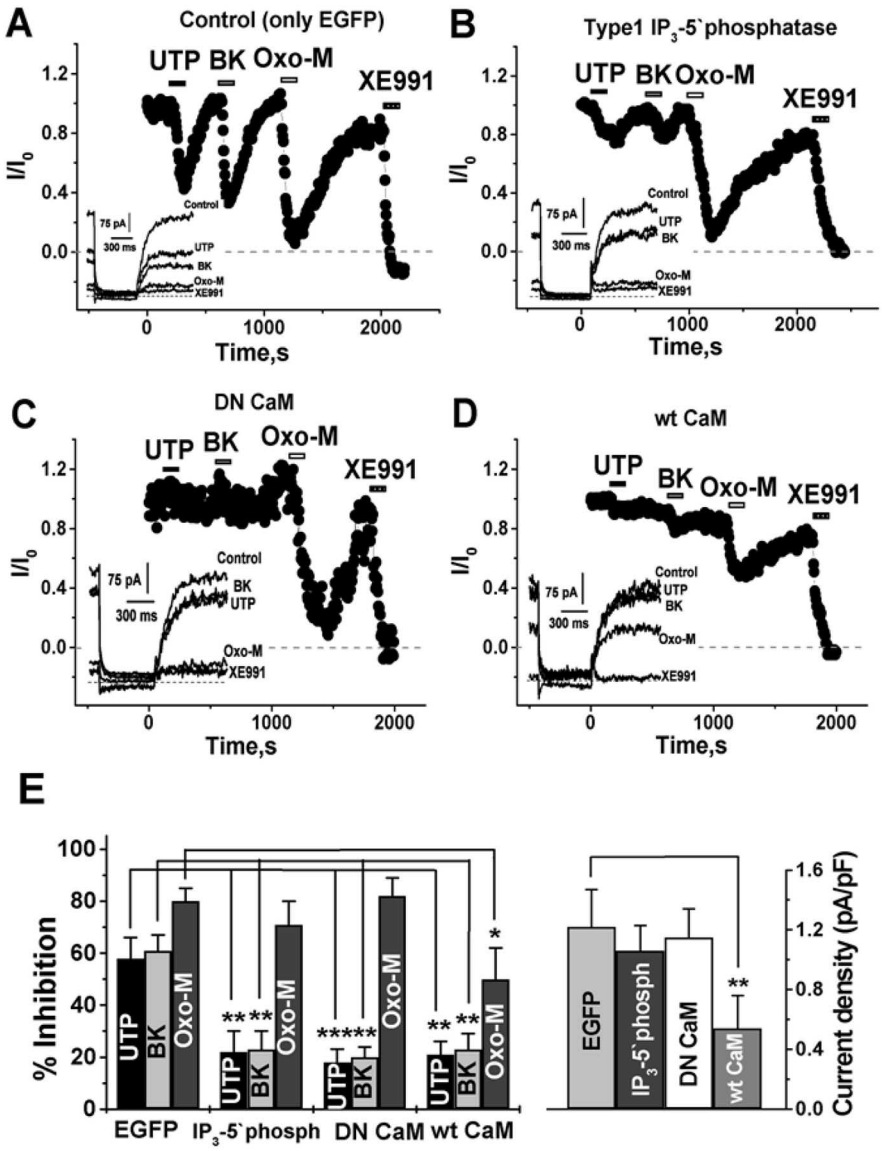

Figure 7. Purinergic suppression of I_M requires cytosolic IP_3 and functional CaM. Plotted are normalized M-current amplitudes quantified as before, from SCG cells transfected using the gene gun with EGFP only (***A***), type 1 IP_3-5′ phosphatase (***B***), DN CaM (***C***), or wt CaM (***D***). UTP (10 μM), BK (250 nM), oxo-M (10 μM), or XE991 (50 μM) were bath applied during the periods shown by the bars. Representative current traces during the experiments are shown in the insets. Bars in ***E*** show summarized data from these experiments for I_M suppression by UTP, BK, and oxo-M (left) or tonic I_M densities (right). *$p < 0.05$; **$p < 0.01$; ***$p < 0.001$.

6% ($p < 0.01$; $n = 4$), and 50 ± 12% ($p < 0.05$; $n = 4$), respectively. The results from the IP_3-P and DN CaM experiments are consistent with our scheme of M-channel regulation, in which there is little tonic modulation at rest via IP_3 or Ca^{2+}/CaM signals. Thus, there should be little effect on tonic I_M densities of lowering resting $[IP_3]$ by transfection of the IP_3-P or occlusion of tonic CaM action by DN CaM overexpression. Conversely, overexpression of wt CaM might greatly amplify tonic Ca^{2+}/CaM inhibition because the IC_{50} of the sensitivity of KCNQ2/3 channels for $[Ca^{2+}]_i$ is ~70 nM, in the range of resting $[Ca^{2+}]_i$, and many more channels will now be tonically bound by Ca^{2+}/CaM (Gamper and Shapiro, 2003). Indeed, this is what we observed (Fig. 7*E*, right). In neurons transfected with EGFP only, IP_3-P, or DN CaM, tonic I_M densities were very similar: 1.2 ± 0.3, 1.1 ± 0.2, and 1.2 ± 0.2 pA/pF ($n = 9$, 6, and 5), respectively. However, in cells overexpressing wt CaM, the tonic I_M density was reduced by more than half, to 0.5 ± 0.2 pA/pF ($p < 0.01$; $n = 4$). Moreover, the reduction of tonic I_M currents in those cells is similar to that produced by BK or UTP, as if Ca^{2+}/CaM-mediated suppression is now tonically strong, consistent with our hypothesis.

The attenuation of muscarinic suppression of I_M in cells overexpressing wt CaM was surprising and somewhat different from the unaffected action of oxo-M in such cells reported previously (Gamper and Shapiro, 2003). One possible reason for the effect involves myrisotylated alanine-rich C kinase substrate (MARCKS) protein that binds to both PIP_2 and Ca^{2+}/CaM in a manner in which binding of the latter is thought to favor unbinding of the former (McLaughlin and Murray, 2005). At low $[Ca^{2+}]_i$, MARCKS can sequester much PIP_2 and then release it on $[Ca^{2+}]_i$ rises. Thus, overexpression of wt CaM may greatly increase the fraction of MARCKS proteins bound by Ca^{2+}/CaM, resulting in increased tonic $[PIP_2]$. Similar to the effect of increasing tonic $[PIP_2]$ by overexpression of phosphatidyl-4-phosphate 5-kinase [PI(4)5-kinase], muscarinic suppression of I_M would then be reduced (Winks et al., 2005). It has been suggested that Ca^{2+}/CaM inhibits M channels by reducing their affinity for PIP_2 (Brown et al., 2007; Gamper and Shapiro, 2007). A second, related, explanation is that overexpression of wt CaM may result in many channels unbinding PIP_2, again resulting in increased tonic $[PIP_2]$ in the vicinity of the channels.

In summary, the IP_3-P and IP_3 sponge data indicate that P2Y receptor-mediated suppression of I_M requires cytosolic IP_3 accumulation. They also provide more evidence for previous conclusions suggesting M-current suppression by BK, but not oxo-M, to also use an IP_3-mediated signal (Cruzblanca et al., 1998). The blockade of purinergic and BK inhibitions in cells overexpressing DN CaM is consistent with those agonists acting via $[Ca^{2+}]_i$ signals in concert with CaM, whose actions are now occluded by the overexpressed DN CaM bound to the channels. Overexpression of wt CaM likely results in most channels already bound by Ca^{2+}/CaM and tonic currents already suppressed before any receptor stimulation, with little additional $IP_3/[Ca^{2+}]_i$-dependent suppression observed. Our data suggest that P2Y receptors in SCG neurons, like B_2 and unlike M_1 receptors, modulate M current through CaM action.

P2Y receptor stimulation does not suppress I_{Ca} unless neuronal Ca^{2+} sensor-1 activity is blocked

Two groups have shown Ca_V2 channels to be regulated by plasma-membrane PIP_2 and its depletion to underlie M_1

receptor-mediated inhibition (Wu et al., 2002; Gamper et al., 2004). Although both muscarinic and bradykinin stimulation provoke robust PLC-mediated PIP_2 hydrolysis in SCG neurons, the former, but not the latter, inhibits PIP_2-sensitive voltage-gated Ca^{2+} channels in those cells (Gamper et al., 2004) (but see Lechner et al., 2005). We suggested this differential action on the Ca^{2+} current (I_{Ca}) to be attributable to receptor-specific depletion of PIP_2, arising from concurrent stimulation of PIP_2 synthesis by bradykinin, but not muscarinic, agonists. In this model, bradykinin, but not muscarinic, stimulation produces IP_3-mediated $[Ca^{2+}]_i$ signals, resulting in acceleration of phosphatidylinositol-4-kinase (PI4)-kinase activity by neuronal Ca^{2+} sensor-1 (NCS-1) (Delmas et al., 2005). Given the similar mode of action of P2Y and B_2 receptors on M current seen in this study, we therefore tested the action of purinergic stimulation on I_{Ca} in SCG cells. As for bradykinin, we found purinergic stimulation to cause little suppression of I_{Ca}. Figure 8*A* shows an example of a neuron studied under perforated-patch voltage clamp under conditions that isolate I_{Ca}. Because stimulation of P2Y receptors has been reported to also activate $G_{o/i}$-mediated signaling pathways (Filippov et al., 2003), SCG cultures were treated overnight with pertussis toxin to isolate $G_{q/11}$-coupled receptor signaling (Beech et al., 1992). Application of neither UTP nor BK caused an appreciable suppression of I_{Ca}, whereas oxo-M produced a robust response in the same cell. In response to application of UTP, BK, or oxo-M, I_{Ca} was suppressed by 4.5 ± 1.0% ($n = 7$), 6.2 ± 0.8% ($n = 7$), and 52.1 ± 4.2% ($n = 7$), respectively (Fig. 8*D*, control). This result suggests that, as for B_2 receptor stimulation, P2Y receptor stimulation does not appreciably lower PIP_2 abundance. We then tested for the involvement of NCS-1-mediated stimulation of PIP_2 synthesis by transfecting a DN mutant that cannot bind Ca^{2+} (Koizumi et al., 2002). In that scenario, cells overexpressing DN NCS-1 should have $[Ca^{2+}]_i$-dependent stimulation of PIP_2 synthesis aborted, allowing PIP_2 abundance to fall during P2Y or BK stimulation and I_{Ca} to be suppressed. Neurons were transfected either with enhanced yellow fluorescent protein (EYFP) only or with EYFP-tagged DN NCS-1. Figure 8, *B* and *C*, show examples from both groups of neurons. In the cell transfected only with EYFP, UTP and BK caused very little suppression of I_{Ca}, but oxo-M induced robust suppression, as in Figure 8*A*. However, in the cell transfected with DN NCS-1, UTP and BK now induced a significant suppression of I_{Ca}, as did oxo-M. These data are summarized in Figure 8*D*. In neurons transfected with EYFP only, application of UTP, BK, and oxo-M suppressed I_{Ca} by 5.8 ± 3.6% ($n = 5$), 8.2 ± 3.2% ($n = 5$), and 53.2 ± 5.7% ($n = 5$). In neurons transfected with DN NCS-1, the suppressions were 31.4 ± 4.7% ($p < 0.01$; $n = 4$), 36.6 ± 6.7% ($p < 0.01$; $n = 4$), and 59.7 ± 8.3% ($n = 4$), respectively. There was no significant effect on tonic I_{Ca} current amplitudes of NCS-1 overexpression. For nontransfected neurons or those transfected with EYFP only or with NCS-1, I_{Ca} densities were 44.4 ± 4.1, 50.4 ± 6.1, and 52.9 ± 3.2 pA/pF ($n =$ 7,5,4), respectively. These results are in accord with our model of selective depletion of PIP_2 by muscarinic, but not purinergic or bradykinin, stimulation. Thus, we suggest that stimulation of both P2Y and B_2 receptors concurrently stimulate PIP_2 synthesis, at least in part, via NCS-1 action, compensating for PIP_2 depletion by PLC activity. With NCS-1 action blocked by overexpression of a DN form, $[PIP_2]$ is allowed to fall during stimulation of either receptor, and stimulation of either now induces significant suppression of I_{Ca}.

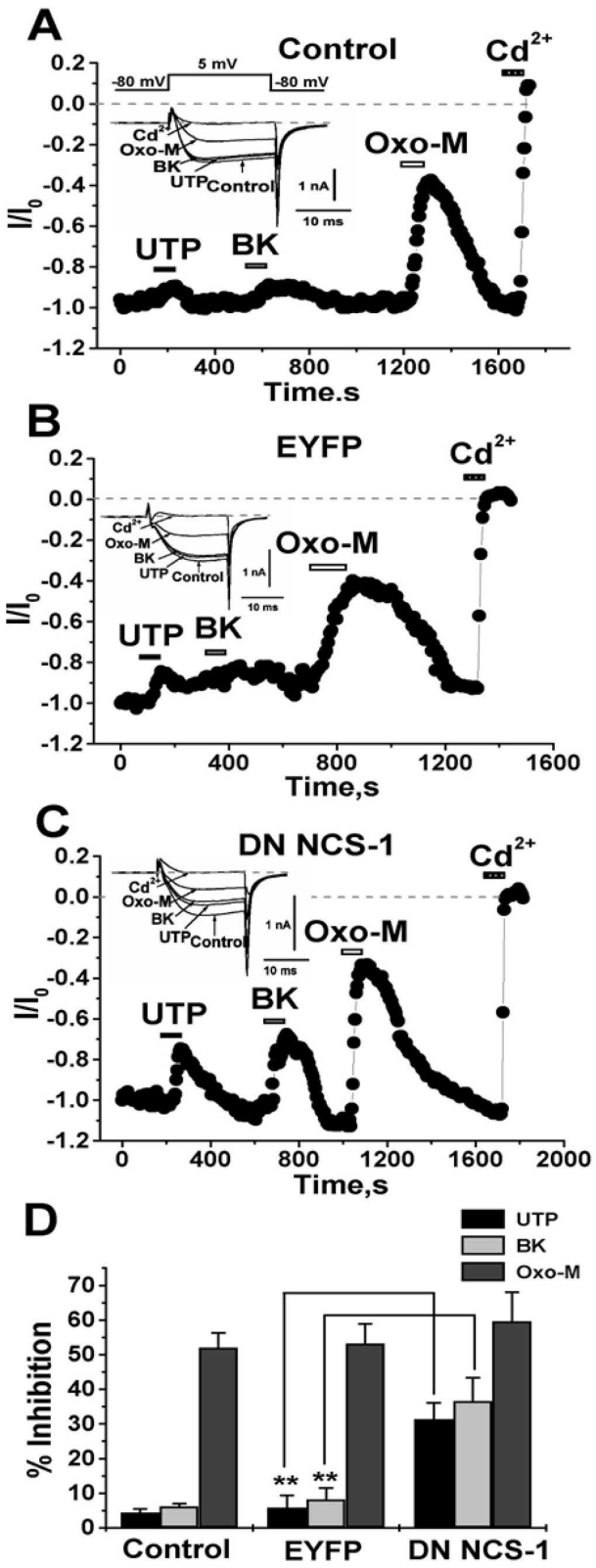

Figure 8. Purinergic and bradykinin stimulation do not suppress I_{Ca} unless NCS-1 activity is blocked. Plotted are normalized I_{Ca} amplitudes from nontransfected SCG neurons (***A***) or those transfected using the gene gun with EYFP only (***B***), or EYFP-tagged DN NCS-1 (***C***) and studied using perforated-patch recordings. SCG cultures were treated overnight with PTX (100 ng/ml) to block $G_{o/i}$-mediated actions. UTP (10 μM), BK (250 nM), oxo-M (10 μM), or $CdCl_2$ (100 μM) were bath applied during the periods shown by the bars. Representative current traces are shown in the insets. ***D***, Bars show summarized data for suppressions of I_{Ca} by UTP, BK, and oxo-M for the three groups of cells. $^{**}p < 0.01$.

Discussion

We suggest that the action of $G_{q/11}$-coupled receptors can be divided into two fundamental modes that have in common PLC activation and hydrolysis of PIP_2. The first mode is based on the widening discovery that many ion channels are regulated by a membrane PIP_2 abundance that can be strongly lowered by PLC (Suh and Hille, 2005). This mechanism seems particularly established for M_1 receptor suppression of M current in sympathetic ganglia and likely for AT_1 receptors as well (Shapiro et al., 1994; Zaika et al., 2006; Suh and Hille, 2007). Both receptor types share the lack of provoked IP_3-mediated $[Ca^{2+}]_i$ signals and dual inhibition of both M-type K^+ and Ca^{2+} channels. The second mode is used by $G_{q/11}$-coupled receptors that do provoke such $[Ca^{2+}]_i$ signals, which then activate multiple Ca^{2+}-binding signaling proteins. The bradykinin B_2 receptor of ganglia cells is the best described in this category. Because of concurrent stimulation of PIP_2 synthesis by bradykinin (Xu et al., 2003) via $[Ca^{2+}]_i$-dependent activation of NCS-1 and acceleration of PI4-kinase activity, PIP_2 levels do not appreciably fall, M channels are inhibited instead by Ca^{2+}/CaM action, and Ca^{2+} channels are little affected (Gamper et al., 2004; Winks et al., 2005; Brown et al., 2007). However, is this action in SCG cells unique to bradykinin? Our work here suggests not and places the purinergic P2Y receptors of these cells in the category using the second mode along with the B_2 receptor. For both, the action of IP_3 receptors is required, CaM functions as the Ca^{2+}-sensor mediating suppression of M current, and Ca^{2+} channels are not modulated. Figure 9 summarizes the bipartite division of $G_{q/11}$-coupled receptor mechanisms hypothesized in sympathetic ganglia cells.

Along with muscarine and several peptides, purinergic agonists were soon identified as regulators of neuronal excitability (Siggins et al., 1977) via depression of M current (Adams et al., 1982; Lopez and Adams, 1989; Tokimasa and Akasu, 1990) in frog sympathetic neurons. The mechanism of action of neuronal P2Y receptors on I_M has been controversial and may depend on precise neuronal type or receptor isoform. Previous work in the rat SCG cells studied here, in which the dominant subtype is likely $P2Y_6$, suggested the requirement for $[Ca^{2+}]_i$ signals (Bofill-Cardona et al., 2000), consistent with our results, but, in frog sympathetic neurons in which the subtype is not clear, the PIP_2-depletion mode is suggested (Stemkowski et al., 2002). Recently, $P2Y_1$ receptor-mediated suppression of M current in hippocampus was studied, and the lack of $[Ca^{2+}]_i$ signals seen during purinergic stimulation in those cells points toward a PIP_2-depletion mechanism there as well. It seems that the basic division between (Filippov et al., 2006) modes of action hinges on the ability of an agonist to provoke $[Ca^{2+}]_i$ signals during receptor stimulation, and the critical factor for induction of such $[Ca^{2+}]_i$ release has been suggested to be colocalization of certain plasma-membrane receptors with endoplasmic reticulum-membrane IP_3 receptors (Delmas et al., 2004). Thus, if IP_3 is produced in the microdomain of the IP_3 receptor, $[Ca^{2+}]_i$ is the relevant signal, and downstream Ca^{2+}-dependent actions of CaM and NCS-1 are initiated; if not, PIP_2 depletion is the mode of action. Perhaps the divergent results in different cells among different P2Y receptor subtypes predict differential localization of receptor isoforms in microdomains containing IP_3 receptors. Alternatively, different neuronal types may use different membrane protein organizations. Although we do not observe suppression of I_{Ca} by bradykinin unless the NCS-1 pathway is blocked (Gamper et al., 2004; this study), Lechner et al. (2005) observe such an inhibition that they ascribe to depletion of PIP_2. The most likely reason for the discrepancy is differential tonic PIP_2 levels, perhaps caused by the different medium/growth conditions used by the two laboratories (Chuang et al., 2001).

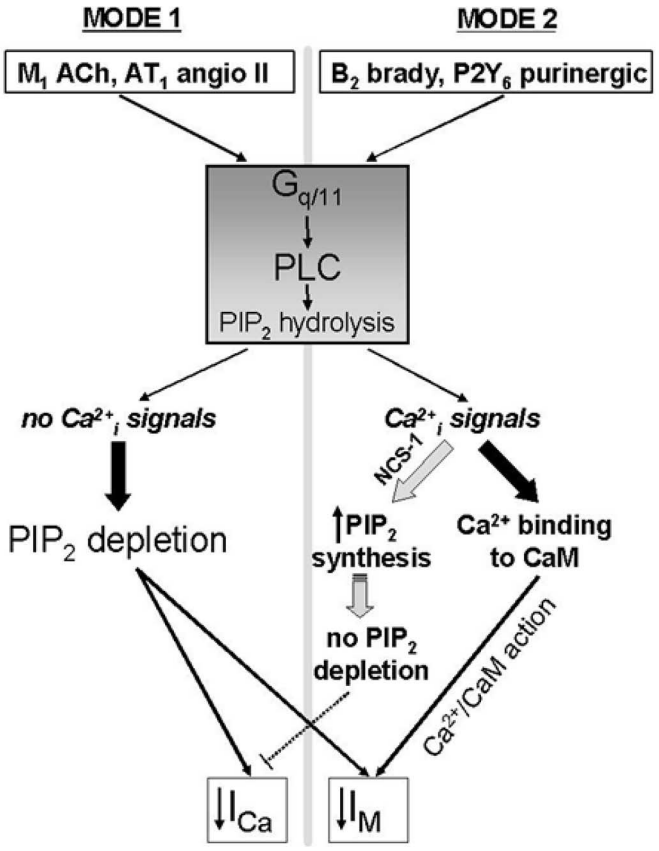

Figure 9. Schematic representation of the two modes of $G_{q/11}$-coupled receptor mechanisms in SCG neurons. Both pathways involve activation of $G_{q/11}$ G-proteins, PLC, and PIP_2 hydrolysis. The "mode 1" pathway suppresses M current (I_M) and Ca^{2+} current (I_{Ca}) attributable to depletion of PIP_2. Mode 1 does not elicit $[Ca^{2+}]_i$ signals. The "mode 2" pathway does elicit $[Ca^{2+}]_i$ signals and concurrently stimulates PIP_2 synthesis via NCS-1. Released Ca^{2+} binds to NCS-1 and to CaM. Ca^{2+}/CaM binds to M channels, resulting in their inhibition.

Filippov and colleagues, using SCG cells as a vehicle for heterologous expression of four different P2Y receptor subtypes, observed an primarily voltage-dependent and PTX-sensitive suppression of I_{Ca} and a wholly PTX-insensitive suppression of I_M by UTP (Filippov et al., 1998, 1999, 2000, 2003). The depression of I_{Ca} seen in those studies had all the hallmarks of the fast "willing-reluctant" type of modulation mediated by $G_{o/i}$-coupled receptors in many neuronal types (Hille, 1994) and none of the characteristics of the slower $G_{q/11}$-mediated pathway typified by M_1 receptors that we ascribe to depletion of PIP_2 (Gamper et al., 2004). We here found purinergic stimulation of PTX-treated neurons to likewise normally have little effect on I_{Ca}. The suppression of I_M in the papers cited above seems similar to that observed by stimulation of native P2Y receptors (Bofill-Cardona et al., 2000; this study), although additional mechanistic information from the heterologous-expression studies is not available. As in the case here using native receptors, stimulation of expressed $P2Y_2$ receptors increased AP firing, consistent with closure of M channels (Filippov et al., 1998). Interestingly, Filippov and colleagues observed little modulation by UTP of either type of channel in nontransfected neurons (which would use native receptors), whereas we observe suppression of I_M in approximately half the SCG cells studied. Perhaps our use of

younger rats (1–2 weeks), and slightly longer culture (2–3 d), provides the explanation. Because colocalization of $P2Y_6$ receptors with IP_3 receptors may underlie the mechanistic specificity described in this study, we appreciate the opportunity to study the actions of the native receptors.

We suggest that stimulation of either B_2 or P2Y receptors does not appreciably deplete membrane PIP_2 attributable, at least in part, to NCS-1-mediated stimulation of PIP_2 synthesis. Such agonist stimulation of PIP_2 synthesis is by now widely documented and has been suggested to be often obligatory to account for the mass of IP_3 produced during PLC activation (Loew, 2007). Independent evidence for receptor-specific depletion of PIP_2 comes from the *tubby* probe that binds PIP_2, but not IP_3 (Santagata et al., 2001). Translocation of *tubby* was minor during bradykinin stimulation in the same cells in which muscarinic translocation was large, but, during acute blockade of PI4-kinase, the translocations were equal (Hughes et al., 2007). In our scheme, blockade of NCS-1 or PI4-kinase activity allows $[PIP_2]$ to fall and I_{Ca} to be suppressed. This scenario presents us with a conundrum, however, because the prevention of IP_3 accumulation by overexpression of the IP_3 sponge or the IP_3-P should prevent the $[Ca^{2+}]_i$ signals that not only activate CaM but also NCS-1, the molecule that we implicate in stimulation of PIP_2 synthesis. With both CaM and NCS-1 activity prevented, why should stimulation of B_2 or P2Y receptors not deplete PIP_2, as by M_1 receptor stimulation? The Hille group has shown some $[Ca^{2+}]_i$ signal (either released from stores or via Ca^{2+} influx) to be necessary for full PLC activity in tsA-201 tissue-culture cells in which overexpression of IP_3-P slowed and weakened diacylglycerol production and KCNQ2/3 channel inhibition by expressed M_1 receptors (Horowitz et al., 2005; Suh et al., 2006). However in the SCG neurons in which muscarinic suppression of M current is strongest, M_1 receptor stimulation does not produce detectable $[Ca^{2+}]_i$ rises (Beech et al., 1991) [unlike stimulation of expressed M_1 receptors in tsA-201 cells (Shapiro et al., 2000)], and we did not observe any effect on muscarinic suppression of I_M of the IP_3 sponge or IP_3-P. Two possible explanations emerge. The first is receptor-specific acceleration of PI(4)5-kinase activity as well, which "virtual cell" modeling suggests is required for compensation of PIP_2 levels in the face of PLC activity (Xu et al., 2003; Loew, 2007). Thus, whereas BK and P2Y receptor triggering may depress M current primarily through IP_3-mediated $[Ca^{2+}]_i$ signals, leading to blockade of I_M suppression when IP_3 accumulation is prevented, the receptor-stimulated acceleration of PIP_2 synthesis may partly be via $[Ca^{2+}]_i$ signals and partly through receptor-specific stimulation of PI(4)5-kinase via an, as yet, unknown pathway. The second possibility is receptor-specific turn on of store-operated Ca^{2+} entry that might require coupling of G-protein-coupled receptors and IP_3 receptor but not IP_3 (Kiselyov et al., 2005). Other aspects of this issue have been discussed recently (Gamper and Shapiro, 2007).

In our comparison among agonists, the effects on excitability generally correlated with degree of M-channel inhibition, although the increase in firing by UTP and BK seemed qualitatively weaker than that by oxo-M. Our finding that neither purinergic nor bradykinin simulation normally suppress I_{Ca} give a hypothesis why this may be so. Simultaneous inhibition of M channels from $G_{q/11}$-coupled M_1 receptor stimulation and of Ca^{2+} channels from combined M_1 and $G_{o/i}$-coupled M_4 receptor stimulation (Hille, 1994) predict a synergistic decrease in K^+ current braking action by the reduced I_M combined with the reduced K_{Ca} conductances from suppression of Ca^{2+} influx, especially likely given the strong role ascribed to the SK channels in controlling the medium afterhyperpolarization (Kawai and Watanabe, 1986; Davies et al., 1996). It is likely that additional mechanisms make a contribution to SFA in these neurons as well. We look forward to a more complete model of simultaneous modulation of multiple ion channels by the same receptor and activation by ionotropic and metabotropic receptors by the same agonist (e.g., acetylcholine, ATP, and glutamate) to understand the multifaceted potential of neurotransmitter-mediated regulation of neuronal function.

References

Adams PR, Brown DA, Constanti A (1982) Pharmacological inhibition of the M-current. J Physiol (Lond) 332:223–262.

Beech DJ, Bernheim L, Mathie A, Hille B (1991) Intracellular Ca^{2+} buffers disrupt muscarinic suppression of Ca^{2+} current and M current in rat sympathetic neurons. Proc Natl Acad Sci USA 88:652–656.

Beech DJ, Bernheim L, Hille B (1992) Pertussis toxin and voltage dependence distinguish multiple pathways modulating calcium channels of rat sympathetic neurons. Neuron 8:97–106.

Bernheim L, Beech DJ, Hille B (1991) A diffusible second messenger mediates one of the pathways coupling receptors to calcium channels in rat sympathetic neurons. Neuron 6:859–867.

Boehm S (1998) Selective inhibition of M-type potassium channels in rat sympathetic neurons by uridine nucleotide preferring receptors. Br J Pharmacol 124:1261–1269.

Bofill-Cardona E, Vartian N, Nanoff C, Freissmuth M, Boehm S (2000) Two different signaling mechanisms involved in the excitation of rat sympathetic neurons by uridine nucleotides. Mol Pharmacol 57:1165–1172.

Borg-Graham L (1991) Modelling the non-linear conductances of excitable membranes. In: Cellular neurobiology: a practical approach (Chad J, Wheal H, eds). Oxford, UK: IRL/Oxford UP.

Brown DA, Hughes SA, Marsh SJ, Tinker A (2007) Regulation of M(Kv7.2/7.3) channels in neurons by PIP_2 and products of PIP_2 hydrolysis: significance for receptor-mediated inhibition. J Physiol (Lond) 582:917–925.

Burnstock G (2006) Purinergic signaling—an overview. Novartis Found Symp 276:26–48; discussion 48–57:275–281.

Calvert JA, Evans RJ (2004) Heterogeneity of P2X receptors in sympathetic neurons: contribution of neuronal $P2X_1$ receptors revealed using knockout mice. Mol Pharmacol 65:139–148.

Calvert JA, Atterbury-Thomas AE, Leon C, Forsythe ID, Gachet C, Evans RJ (2004) Evidence for $P2Y_1$, $P2Y_2$, $P2Y_6$ and atypical UTP-sensitive receptors coupled to rises in intracellular calcium in mouse cultured superior cervical ganglion neurons and glia. Br J Pharmacol 143:525–532.

Chuang HH, Prescott ED, Kong H, Shields S, Jordt SE, Basbaum AI, Chao MV, Julius D (2001) Bradykinin and nerve growth factor release the capsaicin receptor from PtdIns(4,5)P2-mediated inhibition. Nature 411:957–962.

Cooper EC, Jan LY (2003) M-channels: neurological diseases, neuromodulation, and drug development. Arch Neurol 60:496–500.

Cruzblanca H, Koh DS, Hille B (1998) Bradykinin inhibits M current via phospholipase C and Ca^{2+} release from IP_3-sensitive Ca^{2+} stores in rat sympathetic neurons. Proc Natl Acad Sci USA 95:7151–7156.

Davies MP, An RH, Doevendans P, Kubalak S, Chien KR, Kass RS (1996) Developmental changes in ionic channel activity in the embryonic murine heart. Circ Res 78:15–25.

Delmas P, Brown DA (2002) Junctional signaling microdomains: bridging the gap between the neuronal cell surface and Ca^{2+} stores. Neuron 36:787–790.

Delmas P, Brown DA (2005) Pathways modulating neural KCNQ/M (Kv7) potassium channels. Nat Rev Neurosci 6:850–862.

Delmas P, Wanaverbecq N, Abogadie FC, Mistry M, Brown DA (2002) Signaling microdomains define the specificity of receptor-mediated $InsP_3$ pathways in neurons. Neuron 34:209–220.

Delmas P, Crest M, Brown DA (2004) Functional organization of PLC signaling microdomains in neurons. Trends Neurosci 27:41–47.

Delmas P, Coste B, Gamper N, Shapiro MS (2005) Phosphoinositide lipid second messengers: new paradigms for calcium channel modulation. Neuron 47:179–182.

Filippov AK, Webb TE, Barnard EA, Brown DA (1998) $P2Y_2$ nucleotide receptors expressed heterologously in sympathetic neurons inhibit both N-type Ca^{2+} and M-type K^+ currents. J Neurosci 18:5170–5179.

Filippov AK, Webb TE, Barnard EA, Brown DA (1999) Dual coupling of heterologously-expressed rat $P2Y_6$ nucleotide receptors to N-type Ca^{2+} and M-type K^+ currents in rat sympathetic neurones. Br J Pharmacol 126:1009–1017.

Filippov AK, Brown DA, Barnard EA (2000) The P2Y(1) receptor closes the N-type Ca^{2+} channel in neurones, with both adenosine triphosphates and diphosphates as potent agonists. Br J Pharmacol 129:1063–1066.

Filippov AK, Simon J, Barnard EA, Brown DA (2003) Coupling of the nucleotide $P2Y_4$ receptor to neuronal ion channels. Br J Pharmacol 138:400–406.

Filippov AK, Choi RC, Simon J, Barnard EA, Brown DA (2006) Activation of $P2Y_1$ nucleotide receptors induces inhibition of the M-type K^+ current in rat hippocampal pyramidal neurons. J Neurosci 26:9340–9348.

Gamper N, Shapiro MS (2003) Calmodulin mediates Ca^{2+}-dependent modulation of M-type K^+ channels. J Gen Physiol 122:17–31.

Gamper N, Shapiro MS (2006) Exogenous expression of proteins in neurons using the biolistic particle delivery system. Methods Mol Biol 337:27–38.

Gamper N, Shapiro MS (2007) Target-specific PIP_2 signalling: how might it work? J Physiol (Lond) 582:967–975.

Gamper N, Reznikov V, Yamada Y, Yang J, Shapiro MS (2004) Phosphatidylinositol 4,5-bisphosphate signals underlie receptor-specific $G_{q/11}$-mediated modulation of N-type Ca^{2+} channels. J Neurosci 24:10980–10992.

Gamper N, Zaika O, Li Y, Martin P, Hernandez CC, Perez MR, Wang AY, Jaffe DB, Shapiro MS (2006) Oxidative modification of M-type K^+ channels as a mechanism of cytoprotective neuronal silencing. EMBO J 25:4996–5004.

Geiser JR, van Tuinen D, Brockerhoff SE, Neff MM, Davis TN (1991) Can calmodulin function without binding calcium? Cell 65:949–959.

Gu N, Vervaeke K, Hu H, Storm JF (2005) Kv7/KCNQ/M and HCN/h, but not KCa2/SK channels, contribute to the somatic medium after-hyperpolarization and excitability control in CA1 hippocampal pyramidal cells. J Physiol (Lond) 566:689–715.

Halling DB, Aracena-Parks P, Hamilton SL (2006) Regulation of voltage-gated Ca^{2+} channels by calmodulin. Sci STKE 2006:er1.

Hille B (1994) Modulation of ion-channel function by G-protein-coupled receptors. Trends Neurosci 17:531–536.

Hines ML, Carnevale NT (2001) NEURON: a tool for neuroscientists. The Neuroscientist 7:123–135.

Hirose K, Kadowaki S, Tanabe M, Takeshima H, Iino M (1999) Spatiotemporal dynamics of inositol 1,4,5-trisphosphate that underlies complex Ca^{2+} mobilization patterns. Science 284:1527–1530.

Horowitz LF, Hirdes W, Suh BC, Hilgemann DW, Mackie K, Hille B (2005) Phospholipase C in living cells: activation, inhibition, Ca^{2+} requirement, and regulation of M current. J Gen Physiol 126:243–262.

Hughes S, Marsh S, Tinker A, Brown D (2007) PIP_2-dependent inhibition of M-type (Kv7.2/7.3) potassium channels: direct on-line assessment of PIP_2 depletion by G_q-coupled receptors in single living neurons. Pflügers Arch, in press.

Jones S, Brown DA, Milligan G, Willer E, Buckley NJ, Caulfield MP (1995) Bradykinin excites rat sympathetic neurons by inhibition of M current through a mechanism involving B_2 receptors and $G_{aq/11}$. Neuron 14:399–405.

Kawai T, Watanabe M (1986) Blockade of Ca-activated K conductance by apamin in rat sympathetic neurones. Br J Pharmacol 87:225–232.

Kiselyov K, Kim JY, Zeng W, Muallem S (2005) Protein-protein interaction and function of TRPC channels. Pflügers Arch 451:116–124.

Koizumi S, Rosa P, Willars GB, Challiss RA, Taverna E, Francolini M, Bootman MD, Lipp P, Inoue K, Roder J, Jeromin A (2002) Mechanisms underlying the neuronal calcium sensor-1-evoked enhancement of exocytosis in PC12 cells. J Biol Chem 277:30315–30324.

Lawrence JJ, Saraga F, Churchill JF, Statland JM, Travis KE, Skinner FK, McBain CJ (2006) Somatodendritic Kv7/KCNQ/M channels control interspike interval in hippocampal interneurons. J Neurosci 26:12325–12338.

Lechner SG, Hussl S, Schicker KW, Drobny H, Boehm S (2005) Presynaptic inhibition via a phospholipase C- and phosphatidylinositol bisphosphate-dependent regulation of neuronal Ca^{2+} channels. Mol Pharmacol 68:1387–1396.

Loew LM (2007) Where does all the PIP_2 come from? J Physiol (Lond) 582:945–951.

Lopez HS, Adams PR (1989) A G protein mediates the inhibition of the voltage-dependent potassium M current by muscarine, LHRH, substance P and UTP in bullfrog sympathetic neurons. Eur J Neurosci 1:529–542.

Maylie J, Bond CT, Herson PS, Lee WS, Adelman JP (2004) Small conductance Ca^{2+}-activated K^+ channels and calmodulin. J Physiol (Lond) 554:255–261.

McLaughlin S, Murray D (2005) Plasma membrane phosphoinositide organization by protein electrostatics. Nature 438:605–611.

Migliore M, Cook EP, Jaffe DB, Turner DA, Johnston D (1995) Computer simulations of morphologically reconstructed CA3 hippocampal neurons. J Neurophysiol 73:1157–1168.

Moore DJ, Chambers JK, Wahlin JP, Tan KB, Moore GB, Jenkins O, Emson PC, Murdock PR (2001) Expression pattern of human P2Y receptor subtypes: a quantitative reverse transcription-polymerase chain reaction study. Biochim Biophys Acta 1521:107–119.

Peretz A, Degani N, Nachman R, Uziyel Y, Gibor G, Shabat D, Attali B (2005) Meclofenamic acid and diclofenac, novel templates of KCNQ2/Q3 potassium channel openers, depress cortical neuron activity and exhibit anticonvulsant properties. Mol Pharmacol 67:1053–1066.

Peters HC, Hu H, Pongs O, Storm JF, Isbrandt D (2005) Conditional transgenic suppression of M channels in mouse brain reveals functions in neuronal excitability, resonance and behavior. Nat Neurosci 8:51–60.

Rae J, Cooper K, Gates P, Watsky M (1991) Low access resistance perforated patch recordings using amphotericin B. J Neurosci Methods 37:15–26.

Santagata S, Boggon TJ, Baird CL, Gomez CA, Zhao J, Shan WS, Myszka DG, Shapiro L (2001) G-protein signaling through tubby proteins. Science 292:2041–2050.

Shapiro MS, Wollmuth LP, Hille B (1994) Angiotensin II inhibits calcium and M current channels in rat sympathetic neurons via G proteins. Neuron 12:1319–1329.

Shapiro MS, Roche JP, Kaftan EJ, Cruzblanca H, Mackie K, Hille B (2000) Reconstitution of muscarinic modulation of the KCNQ2/KCNQ3 K^+ channels that underlie the neuronal M current. J Neurosci 20:1710–1721.

Shen W, Hamilton SE, Nathanson NM, Surmeier DJ (2005) Cholinergic suppression of KCNQ channel currents enhances excitability of striatal medium spiny neurons. J Neurosci 25:7449–7458.

Siggins GR, Gruol DL, Padjen AL, Formans DS (1977) Purine and pyrimidine mononucleotides depolarise neurones of explanted amphibian sympathetic ganglia. Nature 270:263–265.

Stemkowski PL, Tse FW, Peuckmann V, Ford CP, Colmers WF, Smith PA (2002) ATP-inhibition of M current in frog sympathetic neurons involves phospholipase C but not $InsP_3$, Ca^{2+}, PKC, or Ras. J Neurophysiol 88:277–288.

Suh B, Hille B (2002) Recovery from muscarinic modulation of M current channels requires phosphatidylinositol 4,5-bisphosphate synthesis. Neuron 35:507–520.

Suh BC, Hille B (2005) Regulation of ion channels by phosphatidylinositol 4,5-bisphosphate. Curr Opin Neurobiol 15:370–378.

Suh BC, Hille B (2007) Regulation of KCNQ channels by manipulation of phosphoinositides. J Physiol (Lond) 582:911–916.

Suh BC, Inoue T, Meyer T, Hille B (2006) Rapid chemically induced changes of PtdIns(4,5)P2 gate KCNQ ion channels. Science 314:1454–1457.

Tokimasa T, Akasu T (1990) ATP regulates muscarine-sensitive potassium current in dissociated bull-frog primary afferent neurones. J Physiol (Lond) 426:241–264.

Traub RD, Wong RK, Miles R, Michelson H (1991) A model of a CA3 hippocampal pyramidal neuron incorporating voltage-clamp data on intrinsic conductances. J Neurophysiol 66:635–650.

Uchiyama T, Yoshikawa F, Hishida A, Furuichi T, Mikoshiba K (2002) A novel recombinant hyperaffinity inositol 1,4,5-trisphosphate (IP_3) absorbent traps IP_3, resulting in specific inhibition of IP_3-mediated calcium signaling. J Biol Chem 277:8106–8113.

Vartian N, Moskvina E, Scholze T, Unterberger U, Allgaier C, Boehm S (2001) UTP evokes noradrenaline release from rat sympathetic neurons by activation of protein kinase C. J Neurochem 77:876–885.

Vervaeke K, Gu N, Agdestein C, Hu H, Storm JF (2006) Kv7/KCNQ/M channels in glutamatergic hippocampal axons and their role in regulation of excitability and transmitter release. J Physiol (Lond) 576:235–256.

Wang HS, Pan Z, Shi W, Brown BS, Wymore RS, Cohen IS, Dixon JE, McKinnon D (1998) KCNQ2 and KCNQ3 potassium channel subunits: molecular correlates of the M-channel. Science 282:1890–1893.

Winks JS, Hughes S, Filippov AK, Tatulian L, Abogadie FC, Brown DA, Marsh SJ (2005) Relationship between membrane phosphatidylinositol-4,5-bisphosphate and receptor-mediated inhibition of native neuronal M channels. J Neurosci 25:3400–3413.

Wu L, Bauer CS, Zhen XG, Xie C, Yang J (2002) Dual regulation of voltage-gated calcium channels by PtdIns(4,5)P2. Nature 419:947–952.

Xu C, Watras J, Loew LM (2003) Kinetic analysis of receptor-activated phosphoinositide turnover. J Cell Biol 161:779–791.

Yue C, Yaari Y (2006) Axo-somatic and apical dendritic Kv7/M channels differentially regulate the intrinsic excitability of adult rat CA1 pyramidal cells. J Neurophysiol 95:3480–3495.

Zaczek R, Chorvat RJ, Saye JA, Pierdomenico ME, Maciag CM, Logue AR, Fisher BN, Rominger DH, Earl RA (1998) Two new potent neurotransmitter release enhancers, 10,10-bis(4- pyridinylmethyl)-9(10H)-anthracenone and 10,10-bis(2-fluoro-4- pyridinylmethyl)-9(10H)-anthracenone: comparison to linopirdine. J Pharmacol Exp Ther 285:724–730.

Zaika O, Lara LS, Gamper N, Hilgemann DW, Jaffe DB, Shapiro MS (2006) Angiotensin II regulates neuronal excitability via phosphatidylinositol 4,5-bisphosphate-dependent modulation of Kv7 (M-type) K^+ channels. J Physiol (Lond) 575:49–67.

Zhang H, Craciun LC, Mirshahi T, Rohacs T, Lopes CM, Jin T, Logothetis DE (2003) PIP_2 activates KCNQ channels, and its hydrolysis underlies receptor-mediated inhibition of M currents. Neuron 37:963–975.

Zhou Z, Nehere E (1993) Mobile and immobile calcium buffers in bovine adrenal chromaffin cells. J Physiol 469:245–273.